Reproductive dispersion and damping time scale with life-history speed

Sha Jiang *[1], Harman Jaggi[1], Wenyun Zuo[1], Madan K. Oli[2], Tim Coulson[4], Jean-Michel Gaillard[3], and Shripad Tuljapurkar[1]

[1]Department of Biology, Stanford University, Stanford, CA 94305-5020, USA
[2]Department of Wildlife Ecology and Conservation University of Florida, Gainesville, FL 32611-0430, USA
[3]Laboratoire de Biométrie et Biologie Evolutive, Université Lyon 1, CNRS, UMR 5558, F-69622 Villeurbanne, France
[4]Department of Zoology, University of Oxford, Oxford OX1 3SZ, UK

- Statement of authorship: SJ, HJ performed analyses and writing, WZ, JMG, ST contributed analyses and writing, MO, TC contributed data, ideas and writing.
- Data accessibility statement: No new data were used in this manuscript
- Type of article: Letter
- Keywords: reproductive dispersion, generation time, damping time, life history, slow-fast continuum, biological time
- Number of words in the Abstract: 149
- Number of words in the main text: 4191
- Number of cited references: 59
- Number of tables: 1
- Number of figures: 3 in the main text and 10 in the Appendix

*corresponding author: jiangsha@stanford.edu

Abstract

Generation time has previously been the focus of comparative life history analyses. Here we examine three metrics: generation time T_c, reproductive dispersion S (the distribution of ages of reproduction), and damping time τ (time to converge to stable (st)age distribution). We use data on 633 species of animals and plants, and perform phylogenetically corrected analyses. First we find that S varies allometrically and isometrically with T_c. As a result, τ varies allometrically with either T_c or S but not both. Second, we find a trade-off between τ and S, so that τ does not vary isometrically with T_c. This trade-off is a novel demographic component to the relationship between τ, T_c and S that is otherwise partly determined by their similarity as biological times. Our results indicate that species at the slow end of the slow-fast continuum take longer to converge to stable distribution than species with fast life-histories.

Introduction

Life history traits describe processes such as survival, growth, and reproduction that determine an organism's fitness components and are fundamental to ecological and evolutionary processes, such as biological invasions (Sakai et al. 2001), local extinctions (Silvertown et al. 1996; Jongejans et al. 2008), and species diversification (Chesson 2000). Distinct combinations of life history trait values result in distinct life history strategies (Stearns 1983), and an important goal of life-history theory is to explain the range of variation in strategies exhibited by species (Partridge and Harvey 1988; Hillesheim and Stearns 1992; Roff 1992, 2002; Salguero-Gómez et al. 2016b).

Given the diversity of life history patterns across species, it is notable that theory and empirical evidence suggest that distinct life history strategies are placed along a slow-fast continuum (Stearns 1983, 1992). Species at the slow end of the continuum are characterized by late maturity, low fecundity and long lifespan, which lead to long generation time, and those with the opposite suite of traits occupy the fast end and have short generation time (Franco and Silvertown 1996; Oli 2004; Gaillard et al. 2016; Salguero-Gómez et al. 2016b; Salguero-Gómez 2017). The "speed" of an age-structured life history can be measured by the generation time T_c, the average age of net reproduction, where net reproduction is the product of fertility $m(a)$ and the probability of survival $l(a)$ to age a. A similar generation time can be constructed for stage-structured models (Cochran and Ellner 1992) and age+stage structure (Steiner et al. 2014a). The generation time T_c correlates closely with the position of a species along the slow-fast continuum (Gaillard et al. 2005) and is an important metric for describing variation among life histories (Gamelon et al. 2014; Healy et al. 2019). Of course the generation time does not reflect the age-spread of reproduction in iteroparous species, which is measured by reproductive dispersion (also called demographic dispersion in Tuljapurkar et al. (2009)). Certainly there is no connection in semelparous species that always have zero reproductive dispersion regardless of generation time (Thomas 2013; Crespi and Teo 2002) (note that semelparous individuals may be asynchronous in reproductive timing). But in iteroparous species, the extent of this spread has long been of interest in life history theory (Cole 1954; Trumbo 2013; Hughes 2017; Hautekèete et al. 2001; Varpe and Ejsmond 2018), and is our focus here. Let us quantify the reproductive dispersion by the standard deviation S of the age of net reproduction around the average age T_c (other measures of reproductive dispersion are considered later). The study of reproductive dispersion was made famous by Cole (1954) who explored the difference between semelparity and iteroparity, and there is ongoing interest in the extent of iteroparity (Hautekèete et al. 2001; Trumbo 2013; Hughes 2017; Varpe and Ejsmond 2018). These studies suggest that the reproductive dispersion depends on many factors, including survival at juvenile and adult stages, trade-offs between survival and reproduction, physiological development and regulation, environmental

variability, homeostatic ability, and behavior. In consequence we can argue that, in absence of any structural constraints, there is no systematic covariation across a range of species between the reproductive dispersion S and the average age of reproduction T_c.

However, structural constraints do matter (e.g. allometric constraints that cause all life history traits expressed in mass, time, or length units to change with species-specific body size)(McMahon and Bonner 1983), so we can make an alternative argument for such covariation in iteroparous species. It is known that generation time scales with average adult body mass (M) as $T_c \propto M^{0.25}$ (Millar and Zammuto 1983; Gaillard et al. 2005), like all physiological times (Lindstedt and Calder 1981) or biological times (Lindstedt et al. 1986; Gillooly et al. 2002; Brown et al. 2004; Hamilton et al. 2011). Given that both S and T_c are "biological times", i.e., internal, body-mass-dependent, time scales to which the durations (or rates) of biological events are entrained (Lindstedt et al. 1986), we may expect that reproductive dispersion scales in the same way with body size as generation time, and so the two covary positively and isometrically sensu Huxley and Teissier (1936). But any such relationship between S and T_c is likely to be noisy given the factors mentioned above.

A different perspective on reproductive dispersion comes from its effect on population dynamics. To understand this, consider how a population structure returns to the stable structure after a disturbance. After any such disturbance, reproduction has to fill in any gaps in the population's structure relative to the stable structure, and such gaps will be filled in more rapidly in a species that has a high reproductive dispersion than in a species with low reproductive dispersion. The time scale of population recovery after a disturbance is given by the damping time. For age-structured populations (Keyfitz 1965; Coale 1972; Trussell 1977; Taylor 1979; Tuljapurkar 1982a,b, 1985; Wachter 1991; Caswell 2001), damping time (τ) decreases with the reproductive dispersion (S) but increases with generation time (T_c) (a similar relationship must hold for stage-structured populations). Previous analyses used this result to explore the evolution of life histories (Orzack and Tuljapurkar 1989; Tuljapurkar et al. 2009) but assumed that reproductive dispersion S and generation time T_c can vary independently. While this might hold within species where evolutionary allometry is weak at the best, large body size variation across species should lead to systematic covariation between reproductive dispersion S and generation time T_c that will affect the pattern of variation of damping time τ.

Hence, three hypotheses can be proposed about the association among generation time, reproductive dispersion, and damping time across species that widely differ in size and Baüplan. Under the biological time hypothesis (H1), all three metrics that are expressed in time units should strongly covary positively and isometrically, leaving only a weak and unstructured variation in each metric for a given life history speed. Under the demographic hypothesis (H2), the damping time depends on both reproductive dispersion and generation

time. Lastly (hypothesis H3), both biological time and demographic hypotheses matter, so that all three quantities should covary positively (in partial support of H1), but reproductive dispersion and damping time should be partly decoupled from generation time. For a given life history speed, a trade-off between reproduction dispersion and damping time should be detected (in partial support of H2). Here we describe the results of a test of these hypotheses.

The next section defines reproductive dispersion, generation time, damping time, the (known) analytical approximations, and the data we used. We then analyze the covariation of reproductive dispersion and generation time, and of damping time. The results are based on Phylogenetic Generalized Least Squares (PGLS, Freckleton et al. (2002)) regressions and Phylogenetic Principal Component Analyses (PPCA, Revell (2010)) to account for the effect of phylogeny. We also perform the analysis based on ordinary least squares regression (OLS) and find similar results. The discussion considers the implications of our findings and the possible reasons for them.

Definitions and Data

Reproduction, Dispersion and Damping

We use discrete times and ages. In an age-structured life history (Coale 1972; Caswell 2001; Keyfitz and Caswell 2005), with $m(a)$ and $l(a)$ as defined earlier, the expected lifetime reproduction of a newborn is the net reproductive rate $R_0 = \sum_a l(a)m(a)$. For a cohort (individuals born at the same time), the generation time (the measure we use for life history "speed") is the average age of net reproduction

$$T_c = \frac{\sum_a a\, l(a)m(a)}{R_0},$$

and the spread of reproduction around the mean age T_c is the reproductive dispersion S,

$$S^2 = \frac{\sum_a (a - T_c)^2\, l(a)m(a)}{R_0},$$

Similar definitions for stage-structure are given by Caswell (2001) and for age-and-stage structure by Steiner et al. (2014b), and are used here. Note that there are alternate measures for generation time such as T_b, calculated as weighted mean age of the mothers at childbirth in a population (Gaillard et al. 2005). Our findings hold even if we use T_b in place of T_c for generation time. Other measures of reproductive dispersion such as reproductive span (the difference between age at last reproduction ω and age at first reproduction α) also yield similar results as S. Additionally, when the population is stationary or nearly so, there is a

correlation between evolutionary entropy (Demetrius et al. 2009) and $\log S$.

The dynamics of a structured population are described by a population projection matrix which has a dominant eigenvalue $\lambda_0 = \exp(r_0)$, where r_0 is the population intrinsic rate of increase, and a leading subdominant eigenvalue $\lambda_1 = \exp(r_1 + is_1)$ (where r_1, s_1 are the real and imaginary parts and $i = \sqrt{-1}$). Here r_0 is always larger than r_1 (we assume that the population matrix is irreducible and aperiodic). These eigenvalues define the damping time τ as

$$\tau = \frac{1}{(r_0 - r_1)} > 0. \tag{1}$$

After a disturbance, the population structure approaches stability with time t as cycles around the stable structure whose size (amplitude) decreases over time as $e^{-t/\tau}$. The amplitude of the cycles falls more slowly for a life history with high damping time than a life history with small damping time. Thus the damping time in equation (1) is the time scale of convergence of (st)age-structured populations to the stable (st)age distribution.

An approximate analysis by Wachter (1991) extended earlier work to show that

$$r_0 \approx \frac{\log R_0}{T_c} + \frac{S^2 \, (\log R_0)^2}{2 \, T_c^3}, \tag{2}$$

and

$$r_1 \approx r_0 - \frac{2\pi^2 S^2}{T_c^3}. \tag{3}$$

A similar approximation for r_0 holds in general for structured populations (Steiner et al. 2014b) and we conjecture that in such cases r_1 is similarly given by equation (3).

Using these approximations, the damping time in equation (1) is

$$\tau \simeq \frac{T_c^3}{2\pi^2 \, S^2}. \tag{4}$$

Hence, everything else being constant, damping time τ should increase with generation time T_c, and decrease with increasing age dispersion S of reproduction. If the biological times T_c and S scale perfectly with each other, then damping time τ will increase proportionally with T_c, or alternatively with S.

We also compare the exact damping time τ, calculated from the population projection matrix using equation (1) with the damping time given by the analytical approximation (4). We find that the approximation does qualitatively predict the exact damping time on the log-log scale (see Appendix B and Fig C.10).

Data

We calculate reproductive dispersion in a large number of species covering a wide range of generation times. We use three databases which provide population projection matrices: COMPADRE (v.6.20.5.0) for plants (Salguero-Gómez et al. 2015); COMADRE (v.4.20.5.0) for animals (Salguero-Gómez et al. 2016a); and age-specific data for mammals compiled by Jean-Michel Gaillard (Schindler et al. 2012) and Madan Oli (Oli 2004) (hereafter called GO). These data have been uploaded as a supplement on *github*.

After data checking and cleaning (details in the Appendix A), we have a total of 3865 matrices (689 different species). To carry out phylogenetic generalized least squares (PGLS) and phylogenetic principal component (PPCA) analyses, we begin with a master phylogenetic tree from Open Tree of Life version 12.3 (`https://tree.opentreeoflife.org/about/synthesis-release/v12.3`) and build a phylogenetic tree containing the species in our analysis; we then use the *compute.brlen* function from the R package APE (Paradis and Schliep 2019) to calculate the branch lengths. For species with multiple matrices, we use the median value of reproductive dispersion S to select one matrix for each species as S is more variable than T_c in the data (the mean of CV taken over all species is 0.43 for S and 0.34 for T_c). The resulting dataset includes both phylogenies and life history traits for 633 out of 689 unique species (we could not find phylogenies from the master tree using recorded scientific names for the other 56 species): stage-structured data for 319 species in COMPADRE; stage-structured data for 215 species in COMADRE; age-structured data for 53 species in COMADRE; age-structured data for 75 species in GO. Thus we use these 633 species (633 matrices) for the PGLS analyses as well as PPCA. The data for plants are all stage-structured, whereas animal data are structured by either stage or age (classification discussed in the Appendix A).

In the graphs, results and discussions that follow, note that we standardize the time unit as years. For each species, we compute directly (by standard numerical methods) the life history speed (T_c), the reproductive dispersion (S), and the damping time (τ) from the population projection matrix we retained.

We examine the data and our results in a variety of ways. In the main text, we present PGLS and PPCA results separately for all age-specific data (from GO and COMADRE), stage-specific data for animals (COMADRE), and stage-specific data on plants (COMPADRE). In the Appendix C, we present supplementary figures for PGLS regression for each class of animals and plants.

Results

Generation time and reproductive dispersion

We first analyze the relationship between generation time (T_c) and reproductive dispersion (S), computed as above from the datasets. As shown in Fig 1 for animals (top two panels), and plants (bottom panel), $\log S$ is proportional to $\log T_c$. This conclusion holds within animals and plants, and also within data organized by age-structure alone or stage-structure alone. The relationship between $\log(S)$ and $\log(T_c)$ is strong ($R^2 > 0.8$) and statistically significant ($P \leq 0.001$). The regression of $\log(S)$ versus $\log(T_c)$ in Fig 1 yields slopes between 0.96 and 1.12, all close to the value of 1 that corresponds to isometry. Pagel's λ for animals and plants structured by stage is 0.29 and 0.00, respectively, which indicates that phylogeny has only a weak influence. For animals structured by age, Pagel's λ is 0.63, indicating a moderate influence of phylogeny.

Does a similar relationship between reproductive dispersion and generation time hold for the species within taxonomic classes? We group species by classes, and keep those classes that contain 20 or more species, including *Actinopterygii*, *Aves*, *Mammalia*, and *Reptilia* in animals and *Magnoliopsida* and *Liliopsida* in plants. A strong scaling relationship between reproductive dispersion S and generation time T_c is found in each class. The regression slope between $\log T_c$ and $\log S$ for each class varies but is approximately close to 1 (isometry). Summary statistics for each class such as Pagel's λ and R^2 are reported in the Appendix C (Figs C.1, C.2).

For just age-structured populations we can argue that an increase in reproductive dispersion likely implies a large reproductive span as measured by the difference between age at last reproduction ω and age at first reproduction α. In such cases, the biological time hypothesis implies an allometric and isometric increase in reproductive span ($\omega - \alpha$) with generation time, and indeed we find such a relationship, although noisy (see Appendix Fig C.3).

Figure 1 here

Three time metrics: damping, generation, reproductive dispersion

We next examine how the damping time τ (calculated from the population projection matrix) changes with generation time T_c and reproductive dispersion S, for age or stage structure.

Fig 2 for animals and plants shows that $\log \tau$ is proportional to $\log T_c$ even though the relationship is not isometric. Across species we find that

$$\tau \propto T_c^b, \text{ with } b \text{ between } 0.65 \text{ and } 0.82. \tag{5}$$

The relationship between $\log(\tau)$ and $\log(T_c)$ is statistically significant but noisy, more so for stage-based population models than age-based ones. In addition, the positive relationship holds within classes (see Appendix Fig C.4 and C.5), but is still noisy.

The variability around the main correlation in Fig 2 could be due to the effect of reproductive dispersion, in addition to the inevitable variation due to the effect of sample size or the rarity of some events (e.g., such as deaths of large trees). However, we find that the variability in Fig 2 is largely independent of reproductive dispersion (S) (see Appendix Fig C.6).

Given our previous finding that S scales allometrically with T_c (see comments following equation (4)), we expect that $\log \tau$ is also proportional to $\log S$. This is indeed what we find (see Appendix Fig C.7). These results clearly show that the demographic hypothesis (H2) is false, but only partly support the biological time hypothesis (H1). Although damping time and generation time are positively associated, they are linked with a hypoallometric relationship, meaning that the time to converge to stable (st)age structure increases with generation time but more slowly than if there was the simple proportionality expected under H1.

Figure 2 here

The strong covariation among generation time, reproductive dispersion, and damping time means that we must contend with multicollinearity (Dormann et al. 2013). We therefore turn to a PPCA on the three datasets (i.e. age-structured animals, stage-structured animals, and stage-structured plants). Fig 3 shows the first two principal components (PPC1 and PPC2) for age-structured animals. In the Appendix C we show the corresponding results in Fig C.8 and C.9 for stage-structured animals and plants. Details of the PPCA are presented in Table 1. The results were remarkably consistent across these datasets indicating that the nature of population structure (i.e. age vs. stage) or the type of organism (animal vs. plant) does not influence life history patterns.

As expected under H1, PPC1 captures the positive covariation among the three metrics and accounts for most across-species life history variation. However, this outcome does not fully support H1. First, PPC1 only explains around three-quarter of the total life history variation included in the three metrics (74% for age- and stage-structured animals, 77% for plants). Second, generation time by itself almost entirely determines the time scale corresponding to PPC1 (86% for age-structured animals, 87% for stage-structured animals, and 98% for plants), so we see that PPC1 is aligned with the slow-fast continuum. Both reproductive dispersion and damping time show a substantial variation that is decoupled from the slow-fast continuum, so PPC2 emerges as a second structuring axis of life history variation. This second axis accounts for substantial life history variation (23% for age-structured animals, 26% for stage-structured animals, and 22% for plants) and leaves the third potential

axis to be restricted to noise by accounting only for 3% or less of life history variation (3% for age-structured animals, 0.6% for stage-structured animals, 0.7% for plants). PPC2 describes the trade-off expected under H3 between reproductive dispersion and damping time. Plants and animals differ in the relative contribution to this trade-off between reproductive dispersion and damping time. In animals, reproductive dispersion contributes only slightly more than damping time to PPC2 (loadings for age-structure -0.61 vs. 0.49, for stage-structure -0.57 vs. 0.54), consistently lower than the contribution of these traits to PPC1. In plants, damping time contributes much more than reproductive dispersion to PPC2 (-0.24 vs. 0.85), with a relative contribution much larger than to PPC1.

Figure 3 here

Table 1 here

Discussion

Our first finding here is a robust scaling relationship between reproductive dispersion S and generation time T_c. Across a wide range of species and taxa, S varies allometrically and approximately isometrically with T_c, in partial support of hypothesis H1. This finding implies that species with slow life-histories (characterized by late maturity, low fecundity, and long generation time) typically spread reproduction over a wider age range than those with fast life-histories. A population that has both relatively high T_c and dispersion S is likely better able to time-average risks (e.g., during development, during reproduction). Such bet-hedging strategies may help ride out fluctuations by dispersing the effect over large (st)age classes and have been discussed by Tuljapurkar et al. (2009) and Sæther et al. (2013).

Another consequence of the biological time hypothesis (H1) is that damping time τ should vary allometrically and isometrically with generation time T_c. But we only find that τ is positively correlated with T_c on the log-log scale, with modest effects of reproductive dispersion S. The slope of $\log \tau$ on $\log T_c$ is consistently less than 1, and so the time to converge to stable (st)age structure has a hypoallometric scaling with generation time, which contrasts with the isometric relationship expected under H1.

Nonetheless, this finding implies that species with slow life-histories take a long time to converge to stable structure after disturbances than species with fast life-histories. Our finding greatly extends Capdevila et al. (2020) who argue that the long convergence time (slow recovery rate) of the Asian elephants (*Elephas maximus*) makes them more vulnerable to continuous habitat loss than red squirrels (*Tamiasciurus hudsonicus*). We propose that generation time, a major axis of variation in mammalian life-history tactics (Gaillard et al. 2005), also sets the time scale for response and recovery of species following perturbations.

Alternatively, given that we have found that T_c and S are strongly correlated, we could

state that τ covaries with S on the log-log scale, with small contribution from T_c. Indeed, we find such a relationship, and so hypothesis H2 is rejected because of the covariation of T_c and S. To deal with the collinearity of T_c and S, we use a PPCA.

Our PPCA results provide clear evidence of selective pressure to reduce damping time. The first principal component (PPC1) aligns with the slow-fast continuum. However, we find that PPC2 accounts for about one quarter of overall variation among the three traits analyzed, independent from the slow-fast continuum (PPC1). PPC2 is largely shaped by a trade-off between reproductive dispersion and damping time. This trade-off is pervasive and occurs independently of the population structure or of organisms considered. This trade-off is also consistent with our last hypothesis (H3) which corresponds to a general demographic process that has remained undetected up to now. However, selective pressure against long damping time seems to differ between plants and animals. In animals, reproductive dispersion plays a key role by being weakly coupled to the slow-fast continuum. On the other hand, in plants, damping time is much more strongly decoupled from the slow-fast continuum. We thus propose that in animals an increase in reproductive dispersion limits the long damping time that might accompany a long generation time, whereas in plants an increase of reproductive dispersion has a smaller effect on damping time.

References

Brown, James H et al. (2004). "Toward a metabolic theory of ecology". *Ecology* 85.7, pp. 1771–1789.

Capdevila, Pol, Iain Stott, Maria Beger, and Roberto Salguero-Gómez (2020). "Towards a comparative framework of demographic resilience". *Trends in Ecology & Evolution*.

Caswell, Hal (2001). *Matrix population models: construction, analysis and interpretation*. 2nd. Sunderland, Mass.: Sinauer associates, Sunderland, Mass.

Chesson, Peter (2000). "Mechanisms of maintenance of species diversity". *Annual review of Ecology and Systematics* 31.1, pp. 343–366.

Coale, Ansley Johnson (1972). *The Growth and Structure of Human Populations: A Mathematical Investigation*. Princeton: Princeton University Press.

Cochran, Margaret E and Stephen Ellner (1992). "Simple Methods for Calculating Age-Based Life History Parameters for Stage-Structured Populations: Ecological Archives M062-002". *Ecological monographs* 62.3, pp. 345–364.

Cole, Lamont C (1954). "The population consequences of life history phenomena". *The Quarterly review of biology* 29.2, pp. 103–137.

Crespi, Bernard J and Roy Teo (2002). "Comparative phylogenetic analysis of the evolution of semelparity and life history in salmonid fishes". *Evolution* 56.5, pp. 1008–1020.

Demetrius, Lloyd, Stéphane Legendre, and Peter Harremöes (2009). "Evolutionary entropy: a predictor of body size, metabolic rate and maximal life span". *Bulletin of mathematical biology* 71.4, pp. 800–818.

De Valpine, Perry et al. (2014). "The importance of individual developmental variation in stage-structured population models". *Ecology Letters* 17.8, pp. 1026–1038.

Franco, Miguel and Jonathan Silvertown (1996). "Life history variation in plants: an exploration of the fast-slow continuum hypothesis". *Philosophical Transactions of the Royal Society of London. Series B: Biological Sciences* 351.1345, pp. 1341–1348.

Freckleton, R. P., P. H. Harvey, and M. Pagel (2002). "Phylogenetic Analysis and Comparative Data: A Test and Review of Evidence." *The American Naturalist* 160.6. PMID: 18707460, pp. 712–726. DOI: 10.1086/343873.

Gaillard, Jean-Michel et al. (2005). "Generation time: a reliable metric to measure life-history variation among mammalian populations". *The American Naturalist* 166.1, pp. 119–123.

Gaillard, Jean-Michel et al. (2016). "Life Histories, Axes of Variation in". *The Encyclopedia of Evolutionary Biology*. Ed. by Richard Kliman. Elsevier, Academic Press, pp. 312–323.

Gamelon, Marlène et al. (2014). "Influence of life-history tactics on transient dynamics: a comparative analysis across mammalian populations". *The American Naturalist* 184.5, pp. 673–683.

Gillooly, James. F. et al. (2002). "Effects of size and temperature on developmental time". *Nature* 417.6884, pp. 70–73. DOI: https://doi.org/10.1038/417070a.

Hamilton, Marcus J., Ana D. Davidson, Richard M. Sibly, and James H. Brown (2011). "Universal scaling of production rates across mammalian lineages". *Proceedings of the Royal Society B: Biological Sciences* 278.1705, pp. 560–566. DOI: 10.1098/rspb.2010.1056.

Hautekèete, N-C, Y Piquot, and H Van Dijk (2001). "Investment in survival and reproduction along a semelparity–iteroparity gradient in the Beta species complex". *Journal of Evolutionary Biology* 14.5, pp. 795–804.

Healy, Kevin et al. (2019). "Animal life history is shaped by the pace of life and the distribution of age-specific mortality and reproduction". *Nature ecology & evolution* 3.8, pp. 1217–1224.

Hillesheim, Elke and Stephen C Stearns (1992). "Correlated responses in life-history traits to artificial selection for body weight in Drosophila melanogaster". *Evolution* 46.3, pp. 745–752.

Hughes, Patrick William (2017). "Between semelparity and iteroparity: empirical evidence for a continuum of modes of parity". *Ecology and evolution* 7.20, pp. 8232–8261.

Huxley, Julian S and Georges Teissier (1936). "Terminology of relative growth". *Nature* 137.3471, pp. 780–781.

Jongejans, Eelke, Natasha De Vere, and Hans de Kroon (2008). "Demographic vulnerability of the clonal and endangered meadow thistle". *Plant Ecology* 198.2, pp. 225–240.

Keyfitz, Nathan and Hal Caswell (2005). *Applied mathematical demography*. Vol. 47. Springer.

Keyfitz, Nathan. (1965). "The Intrinsic Rate of Natural Increase and the Dominant Root of the Projection Matrix". *Population Studies* 18.3, pp. 293–308.

Lindstedt, SL and WA Calder III (1981). "Body size, physiological time, and longevity of homeothermic animals". *The Quarterly Review of Biology* 56.1, pp. 1–16.

Lindstedt, Stan L, Brian J Miller, and Steven W Buskirk (1986). "Home range, time, and body size in mammals". *Ecology* 67.2, pp. 413–418.

McMahon, Thomas A and John Tyler Bonner (1983). *On size and life*. Scientific American Library, New York.

Millar, John S and Richard M Zammuto (1983). "Life histories of mammals: an analysis of life tables". *Ecology* 64.4, pp. 631–635.

Oli, Madan K (2004). "The fast–slow continuum and mammalian life-history patterns: an empirical evaluation". *Basic and Applied Ecology* 5.5, pp. 449–463.

Orzack, Steven Hecht and Shripad Tuljapurkar (1989). "Population dynamics in variable environments. VII. The demography and evolution of iteroparity". *The American Naturalist* 133.6, pp. 901–923.

Paradis, Emmanuel and Klaus Schliep (2019). "ape 5.0: an environment for modern phylogenetics and evolutionary analyses in R". *Bioinformatics* 35.3, pp. 526–528.

Partridge, Linda and Paul H Harvey (1988). "The ecological context of life history evolution". *Science* 241.4872, pp. 1449–1455.

Revell, Liam J (2010). "Phylogenetic signal and linear regression on species data". *Methods in Ecology and Evolution* 1.4, pp. 319–329.

Roff, Derek A (2002). *Life history evolution*. 576.54 R6. Sinauer, Sunderland.

— (1992). *The Evolution of Life Histories: Theory and Analysis*. Chapman and Hall, New York.

Sæther, Bernt-Erik et al. (2013). "How life history influences population dynamics in fluctuating environments". *The American Naturalist* 182.6, pp. 743–759.

Sakai, Ann K et al. (2001). "The population biology of invasive species". *Annual review of ecology and systematics* 32.1, pp. 305–332.

Salguero-Gomez, Roberto and Joshua B Plotkin (2010). "Matrix dimensions bias demographic inferences: implications for comparative plant demography". *The American Naturalist* 176.6, pp. 710–722.

Salguero-Gómez, Roberto (2017). "Applications of the fast–slow continuum and reproductive strategy framework of plant life histories". *New Phytologist* 213.4, pp. 1618–1624.

Salguero-Gómez, Roberto et al. (2015). "The COMPADRE Plant Matrix Database: an open online repository for plant demography". *Journal of Ecology* 103.1, pp. 202–218.

Salguero-Gómez, Roberto et al. (2016a). "COMADRE: a global data base of animal demography". *Journal of Animal Ecology* 85.2, pp. 371–384.

Salguero-Gómez, Roberto et al. (2016b). "Fast–slow continuum and reproductive strategies structure plant life-history variation worldwide". *Proceedings of the National Academy of Sciences* 113.1, pp. 230–235.

Schindler, Susanne, Shripad Tuljapurkar, Jean-Michel Gaillard, and Tim Coulson (2012). "Linking the population growth rate and the age-at-death distribution". *Theoretical Population Biology*.

Silvertown, Jonathan, Miguel Franco, and Eric Menges (1996). "Interpretation of elasticity matrices as an aid to the management of plant populations for conservation". *Conservation Biology* 10.2, pp. 591–597.

Stearns, Stephen C (1983). "The influence of size and phylogeny on patterns of covariation among life-history traits in the mammals". *Oikos* 41.2, pp. 173–187.

— (1992). *The Evolution of life histories*. Oxford: Oxford University Press.

Steiner, Ulrich K, Shripad Tuljapurkar, and Tim Coulson (2014a). "Generation time, net reproductive rate, and growth in stage-age-structured populations". *The American Naturalist* 183.6, pp. 771–783.

— (2014b). "Generation time, net reproductive rate, and growth in stage-age-structured populations". *The American Naturalist* 183.6, pp. 771–783.

Taylor, Fritz (1979). "Convergence to the stable age distribution in populations of insects". *The American Naturalist* 113.4, pp. 511–530.

Thomas, Howard (2013). "Senescence, ageing and death of the whole plant". *New Phytologist* 197.3, pp. 696–711.

Trumbo, Stephen T (2013). "Maternal care, iteroparity and the evolution of social behavior: a critique of the semelparity hypothesis". *Evolutionary Biology* 40.4, pp. 613–626.

Trussell, T James (1977). "Determinants of roots of Lotka's equation". *Mathematical Biosciences* 36.3-4, pp. 213–227.

Tuljapurkar, Shripad (1982a). "Population dynamics in variable environments. II. Correlated environments, sensitivity analysis and dynamics". *Theoretical Population Biology* 21.1, pp. 114–140.

— (1982b). "Population Dynamics in Variable Environments. III. Evolutionary Dynamics of r-Selection." *Theoretical Population Biology* 21.1, pp. 141–165.

— (1985). "Population dynamics in variable environments. VI. Cyclical environments". *Theoretical Population Biology* 28.1, pp. 1–17.

Tuljapurkar, Shripad, Jean-Michel Gaillard, and Tim Coulson (2009). "From stochastic environments to life histories and back". *Philosophical Transactions of the Royal Society B: Biological Sciences* 364.1523, pp. 1499–1509.

Varpe, Øystein and Maciej J Ejsmond (2018). "Semelparity and iteroparity". *Natural history of crustacea* 5, pp. 97–124.

Wachter, Kenneth W (1991). "Elusive Cycles: Are there dynamically possible Lee-Easterlin models for US births?" *Population Studies* 45.1, pp. 109–135.

Figure

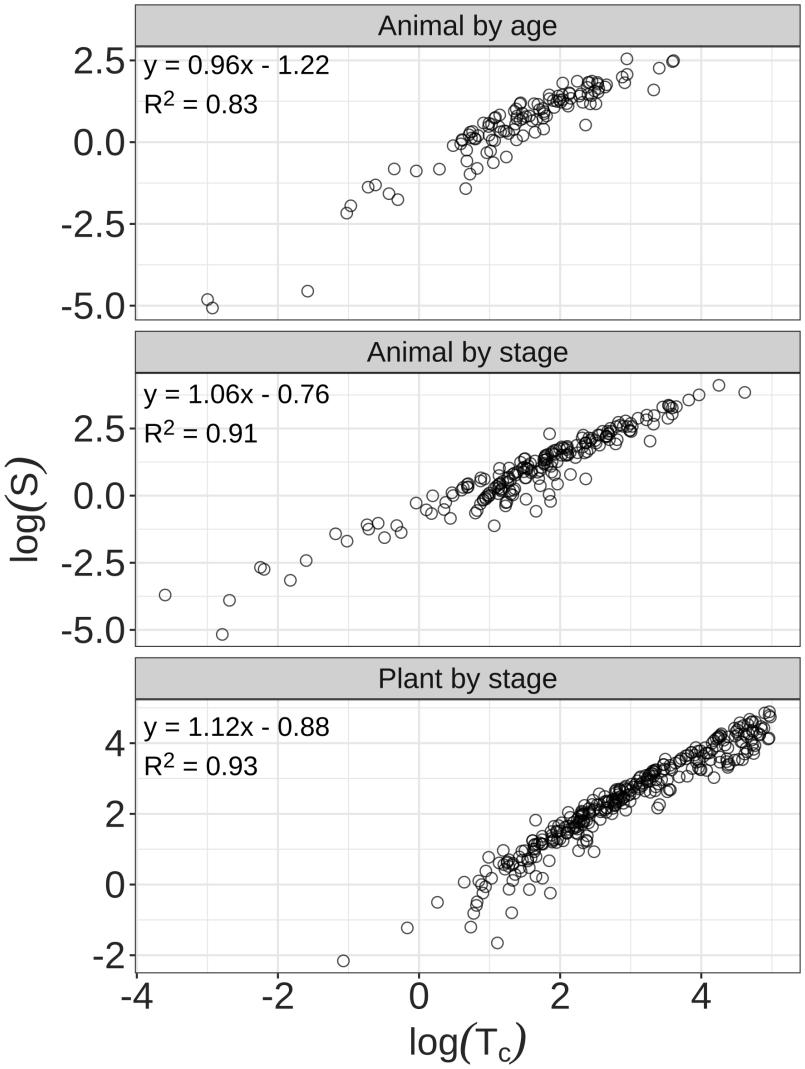

Figure 1: Reproductive dispersion (S) versus generation time (T_c) on a log-log scale. Time unit is years. Upper panel, age-structured animal data from COMADRE and GO; middle panel, stage-structured animal data from COMADRE; bottom panel, stage-structured plant data from COMPADRE. Each panel displays the fitted model and its coefficient of determination (R^2) based on PGLS regression. P-value in each panel is less than 0.001. The 95% confidence interval for the regression slope is [0.92, 1.00] for the upper panel, [1.04, 1.09] for the middle panel and [1.11, 1.14] for the bottom panel. Pagel's λ is 0.63, 0.29 and 0.00 for the upper, middle and bottom panels respectively.

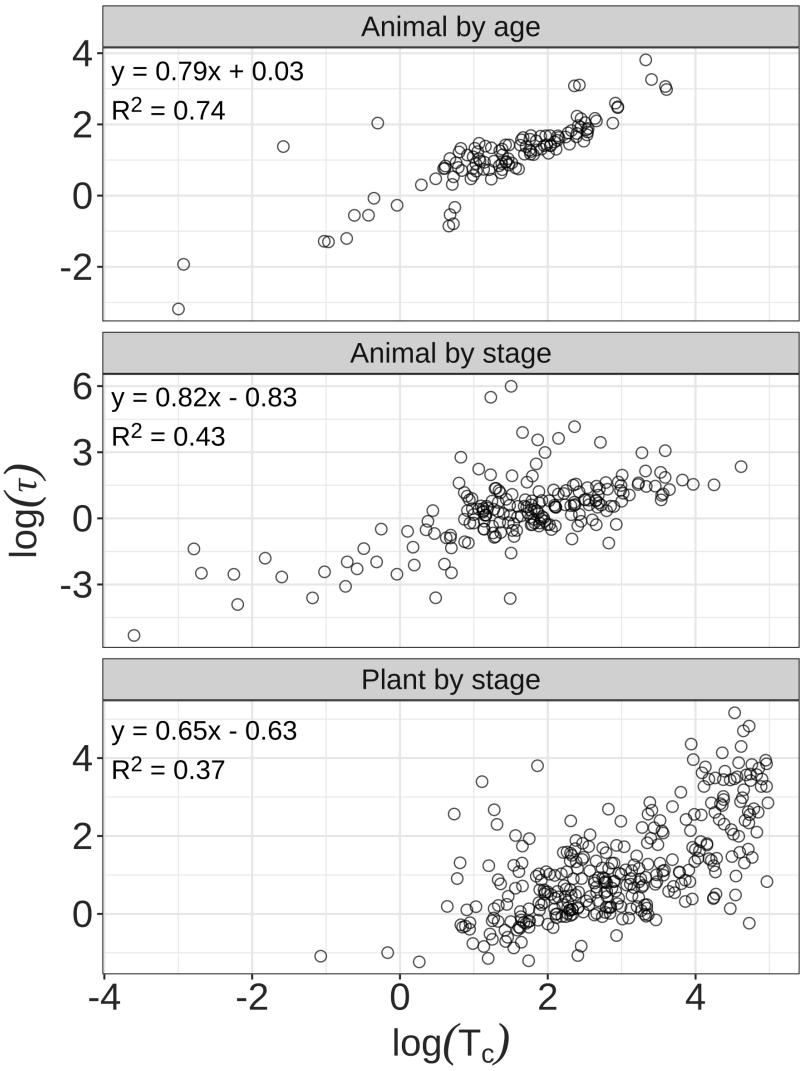

Figure 2: Damping time (τ) versus generation time (T_c) on a log-log scale. Damping time (τ) is calculated directly from each population projection matrix. Time unit is years. Upper panel, age-structured animal data from COMADRE (circles) and GO (crosses); middle panel, stage-structured animal data from COMADRE; bottom panel, stage-structured plant data from COMPADRE. Each panel displays the fitted model and its coefficient of determination (R^2) based on PGLS regression. P-value in each panel is less than 0.001. The 95% confidence interval for the regression slope of each panel is [0.74, 0.83] for the upper panel, [0.75, 0.89] for the middle panel and [0.61, 0.70] for the bottom panel. Pagel's λ is 0.00, 0.13 and 0.27 for the upper, middle and bottom panels respectively.

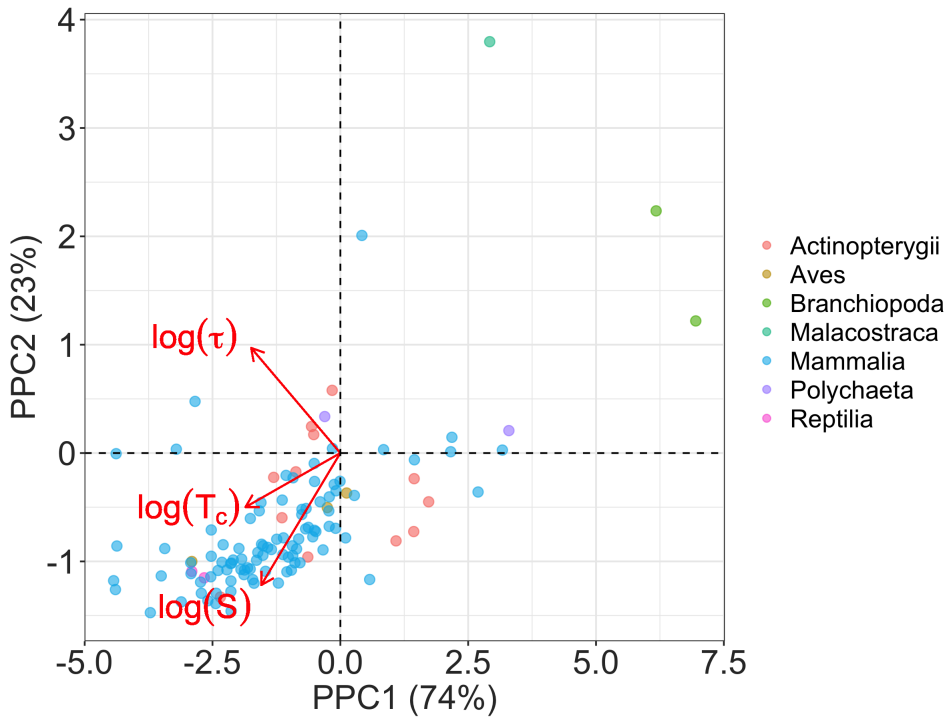

Figure 3: Phylogenetic principal component analysis (PPCA) of reproductive dispersion (S), generation time (T_c) and damping time (τ) on a log scale for age-structured animals. Arrow length indicates the loading of each life-history trait onto PCA axes. Points represent the position of species along the phylogeneticly corrected principal component (PPC)1 and 2, and are colored by Class. Numbers in parentheses on both axes represent the proportion of variance explained by the corresponding PPC. Results for stage-structured animals and plants can be found in the Appendix C.

Table

Table 1: Loadings from a phylogenetic principal component analysis (PPCA)

Dataset		**Principal component**	
		PPC1	PPC2
Animal by age	Metric		
	$log(T_c)$	-0.93	-0.25
	$log(S)$	-0.77	-0.61
	$log(\tau)$	-0.87	0.49
	Proportion of variance	74%	23%
	Cumulative proportion	74%	97%
Animal by stage	Metric		
	$log(T_c)$	0.93	-0.34
	$log(S)$	0.82	-0.57
	$log(\tau)$	0.84	0.54
	Proportion of variance	74%	26%
	Cumulative proportion	74%	99%
Plant by stage	Metric		
	$log(T_c)$	-0.99	-0.07
	$log(S)$	-0.97	-0.24
	$log(\tau)$	-0.53	0.85
	Proportion of variance	77%	22%
	Cumulative proportion	77%	99%

Appendix

A Supplementary Information on Data

For COMPADRE (v.6.20.5.0) and COMADRE (v.4.20.5.0) database, there are initially 8925 matrices (759 species) and 2275 matrices (415 species), respectively. Then we conduct a series of data cleaning to prepare the dataset for the analysis.

A.1 Data classification for age- and stage-structured matrices

The COMADRE and COMPADRE database consists of three criteria to indicate whether the population projection matrix contains (st)ages based on size (MatrixCriteriaSize), devel-

opment (MatrixCriteriaOntogeny), age (MatrixCriteriaAge). We get a rough classification of age and stage-structured data after removing 'NA' in the three criteria. If MatrixCriteriaSize == "No" & MatrixCriteriaAge == "Yes" & MatrixCriteriaOntogeny == "No", it's considered as age-structured data, otherwise it's stage-structured data.

For COMPADRE, we only consider stage-structured data for the analysis. For age-structured data in COMADRE, we further check the intersection of last row and last column in the survival matrix. If the value is zero, then we classify it as a age-structured data; if it is non-zero, then classify it as stage-structured data considering that some individuals will survive beyond the last age observed.

A.2 Filters used before calculation

Using the flags in the dataset, we exclude data with missing values in vital rates (i.e, no NA's in the matrices); ensure the survival probability is always less than 1 for the last (st)age and less than or equal to 1 for other (st)ages; ensure the survival probability for the last age/stage is always less than 1; ensure the fecundity was measured in the study; remove data from one unclear source (Master thesis with no title and author name); remove semelparous species *Oncorhynchus tshawytscha* (Chinook salmon), Bacteria (*Spirochaetes*) and Virus (*lentivirus*).

We keep those fertility matrices that have non-zero elements only on the first row to ensure offspring are born into the first (st)age. We eliminate those matrices with non-zero cloning data since we do not analyse clonal mode of reproduction. To standardize the life-history traits to units of year based on the values of projection intervals, we only keep matrices where the projection interval is non-zero. For data that have mixed male and female population projection matrices in one matrix, marked as StudiedSex == "M/F - Males and females separately in the same population matrix model" in the database, we separate and check them individually according to their source papers.

For age-structured data in COMADRE, we further ensure survival matrix should have non-zero value only in the sub-diagonal; ensure that the fertility matrix has more than 1 non-zero value in the first row to allow for dispersion of reproductive events.

A.3 Filters used during and after calculation

For stage-structured data in both COMADRE and COMPADRE, we remove matrices where (I-U) inverse does not exist (where I is the Identity matrix and U is the survival matrix) to enable the calculation. Besides, considering the biological realisticity, we remove unlikely values by ensuring $\log(T_c) < 5$, $\log(S) > -15$, and $\log(\tau) < 15$.

A.4 Matrices used for PGLS analysis

We then combine our computed life-history traits (generation time, reproductive dispersion and damping time) with the phylogenetic tree we build based on the master phylogenetic tree from Open Tree of Life version 12.3 (https://tree.opentreeoflife.org/about/synthesis-release/v12.3). For several species we had multiple matrices, we use the median value of age-dispersion S to select one matrix for each species as S was much more variable than T_c in the data (the mean of CV within each species is 0.43 for S and 0.34 for T_c). The resulting dataset includes both phylogenies and life history traits for 633 out of 689 unique species (we could not find phylogenies from the master tree using recorded scientific names for the other 56 species). Thus we used these 633 species (633 matrices) for the PGLS analyses: stage-structured data for 319 species in COMPADRE; stage-structured data for 215 species in COMADRE; age-structured data for 53 species in COMADRE; age-structured data for 75 species in GO.

A.5 Limitations

Small population sizes may lead to biased estimates of vital rates. In some populations that have long-lived stage(s), such as trees, the numbers of deaths to large individuals observed during the study period may be small so the corresponding estimated survival rates may be artificially high. Consequently, studies that incorporate both age and stage structure will be important (de Valpine et al. 2014). Matrix dimensionality is taken from the data, but is known to influence the life-history traits calculated (Salguero-Gomez and Plotkin 2010).

B How Good is the Analytical Approximation?

Recall that equation (4) approximates damping time τ in terms of the ratio T_c^3/S^2. To evaluate this approximation, we compare the exact damping time τ (calculated directly from the population projection matrix) and the damping time τ given by the analytical approximation. On a log-log scale, we find that the analytical approximation does qualitatively predict the exact damping time, indicating a statistically significant correlation between them (see Appendix Fig C.10). In general, the damping time from the approximation is smaller than the damping time calculated from data. Compared to plants, the analytical approximation for animals is better because the OLS regression for animals has a slope close to 1 (0.94 for age-structured animals, 0.84 for stage-structured animals, and 0.63 for plants) and a large R^2 (0.71 for age-structured animals, 0.79 for stage-structured animals, and 0.54 for plants). This could be because the approximation ignores higher moments of the distribution of reproduction, which may be significant for plants and animals with stage-based dynamics.

C Figure

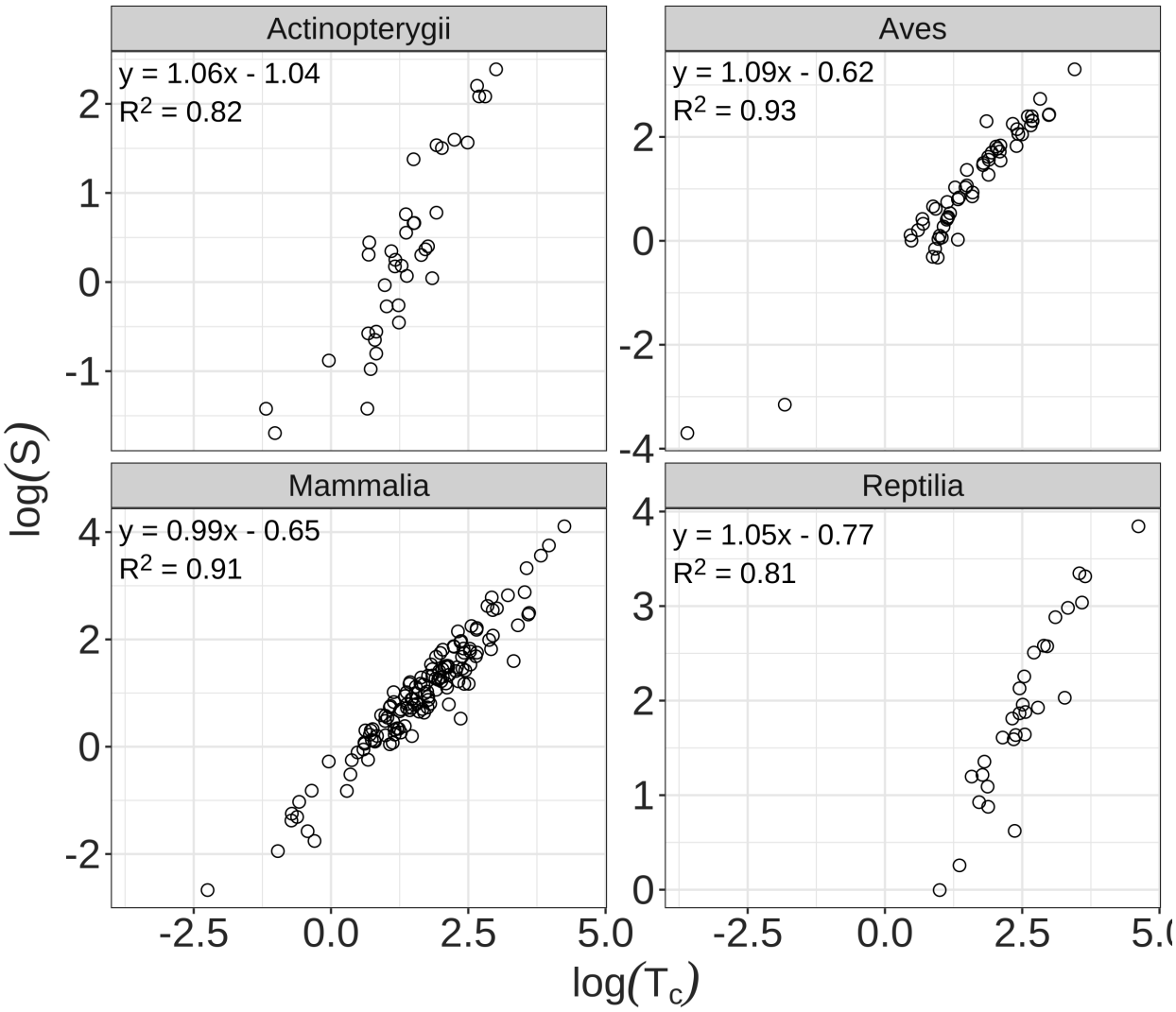

Figure C.1: Class-wise plots for reproductive dispersion (S) versus generation time (T_c) on a log scale for animals. The unit of time is years. Each panel corresponds to a Class. On the top left of each panel, we also present the fitted model and its coefficient of determination (R^2) based on PGLS regression. P-value in each panel is less than 0.001. The 95% confidence interval for the regression slope and the value of Pagel's λ are [0.98, 1.14] and 0.50 for *Actinopterygii*, [1.05, 1.13] and 0.00 for *Aves*, [0.96, 1.01] and 0.01 for *Mammalia*, [0.95, 1.14] and 0.01 for *Reptilia*.

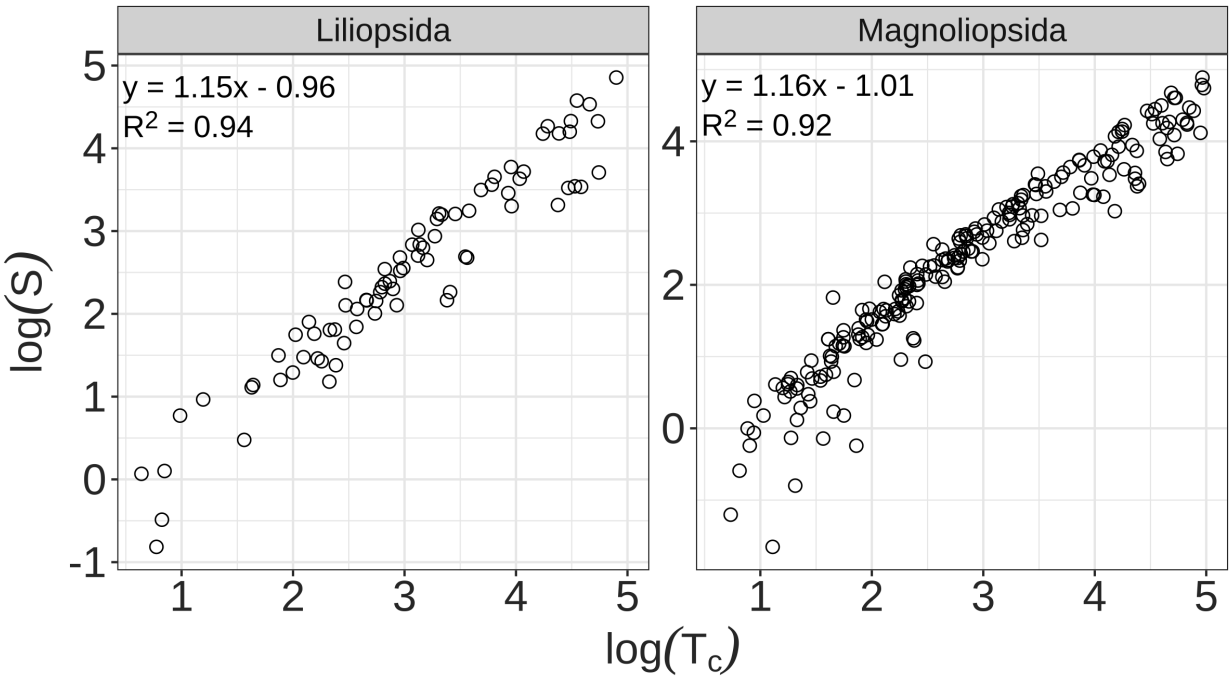

Figure C.2: Class-wise plots for reproductive dispersion S versus generation time T_c on a log scale for plants. The unit of time is years. Each panel corresponds to a Class. On the top left of each panel, we also present the fitted model and its coefficient of determination (R^2) based on PGLS regression. P-value in each panel is less than 0.001. The 95% confidence interval for the regression slope and the value of Pagel's λ are [1.11, 1.18] and 0.83 for *Liliopsida*, [1.13, 1.18] and 0.05 for *Magnoliopsida*.

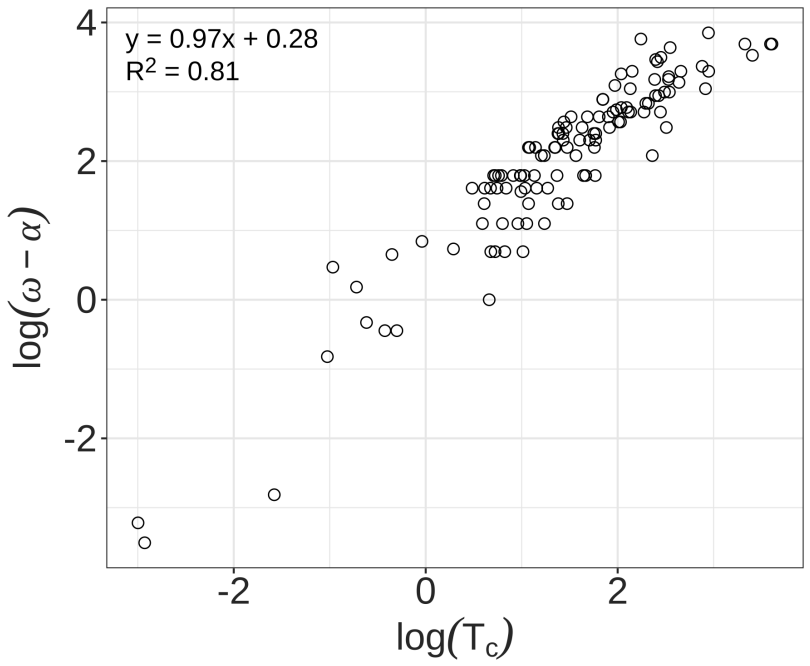

Figure C.3: Reproductive span ($\omega - \alpha$) versus generation time (T_c) on a log scale for age-structured animals. The unit of time is years. On the top left, we also present the fitted model and its coefficient of determination (R^2) based PGLS regression. P-value is less than 0.01. The 95% confidence interval for the regression slope and the value of Pagel's λ are [0.92, 1.01] and 0.60.

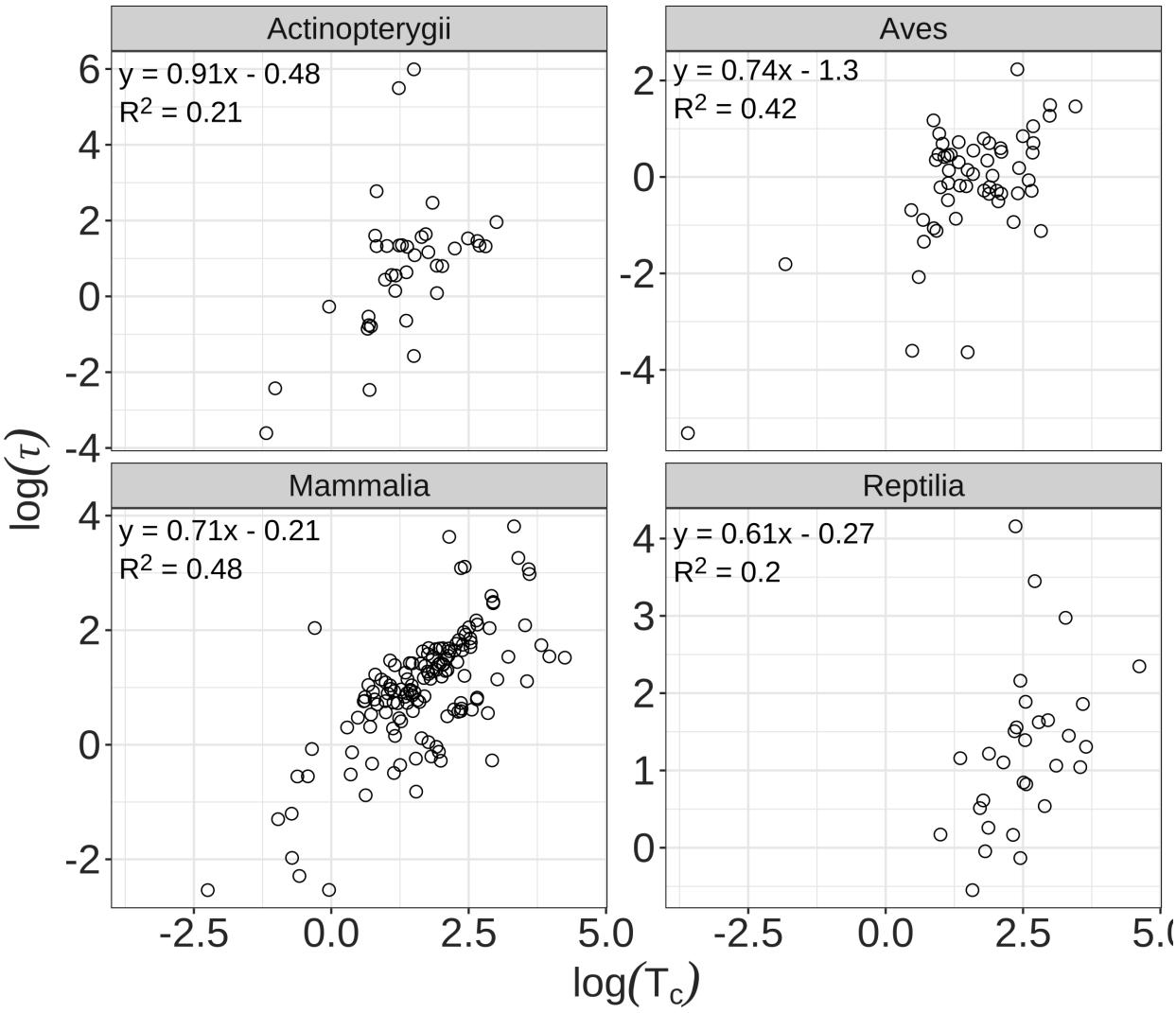

Figure C.4: Class-wise plots for damping time (τ) versus generation time (T_c) on a log scale for animals. It should be noted that the damping time (τ) presented here is the exact value calculated from population projection matrix instead of the approximation in equation (4). The unit of time is years. Each panel corresponds to a Class. On the top left of each panel, we also present the fitted model and its coefficient of determination (R^2) based on PGLS regression. P-value in each panel is less than 0.01, except for *Reptilia* (P = 0.01). The 95% confidence interval for the regression slope and the value of Pagel's λ are [0.62, 1.20] and 0.52 for *Actinopterygii*, [0.62, 0.86] and 0.00 for *Aves*, [0.65, 0.77] and 0.00 for *Mammalia*, [0.38, 0.84] and 0.00 for *Reptilia*.

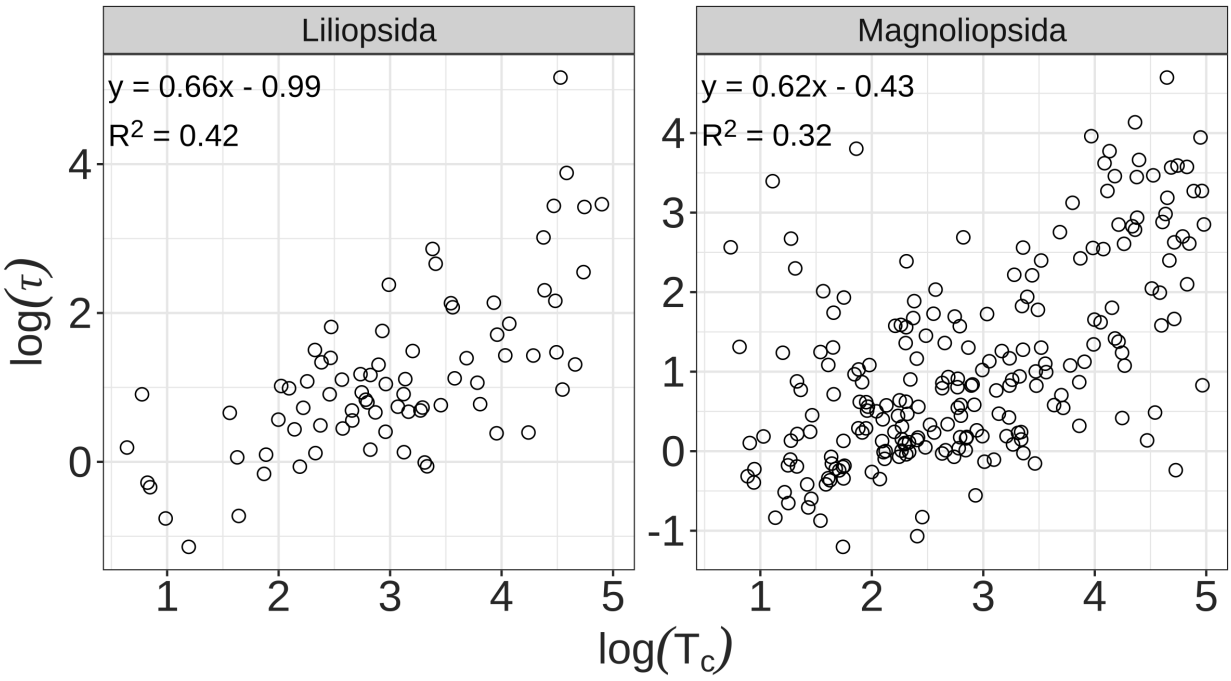

Figure C.5: Class-wise plots for damping time (τ) versus generation time (T_c) on a log scale for plants. The unit of time is years. Each panel corresponds to a Class. It should be noted that the damping time (τ) presented here is the exact value calculated from population projection matrix instead of the approximation in equation (4). On the top left of each panel, we also present the fitted model and its coefficient of determination (R^2) based on PGLS regression. P-value in each panel is less than 0.01. The 95% confidence interval for the regression slope and the value of Pagel's λ are [0.57, 0.74] and 0.45 for *Liliopsida*, [0.56, 0.68] and 0.12 for *Magnoliopsida*.

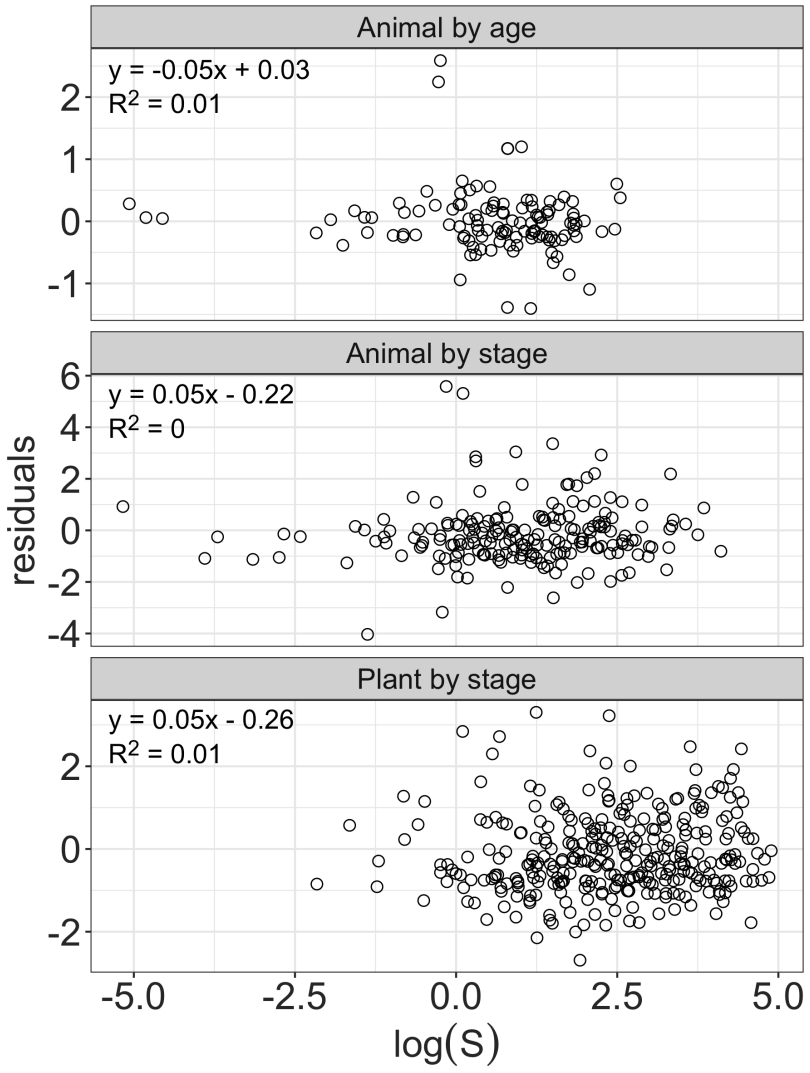

Figure C.6: Residuals of the PGLS model of $\log(\tau)$ and $\log T_c$ versus reproductive dispersion in a log scale ($\log(S)$). On the top left of each panel, we also present the fitted model and its coefficient of determination (R^2) based on ordinary least squares regression (OLS). P-value in each panel is larger than 0.1. The 95% confidence interval for the regression slope is [-0.09, -0.01] for the upper panel, [-0.01, 0.11] for the middle panel and [0.01, 0.09] for the bottom panel.

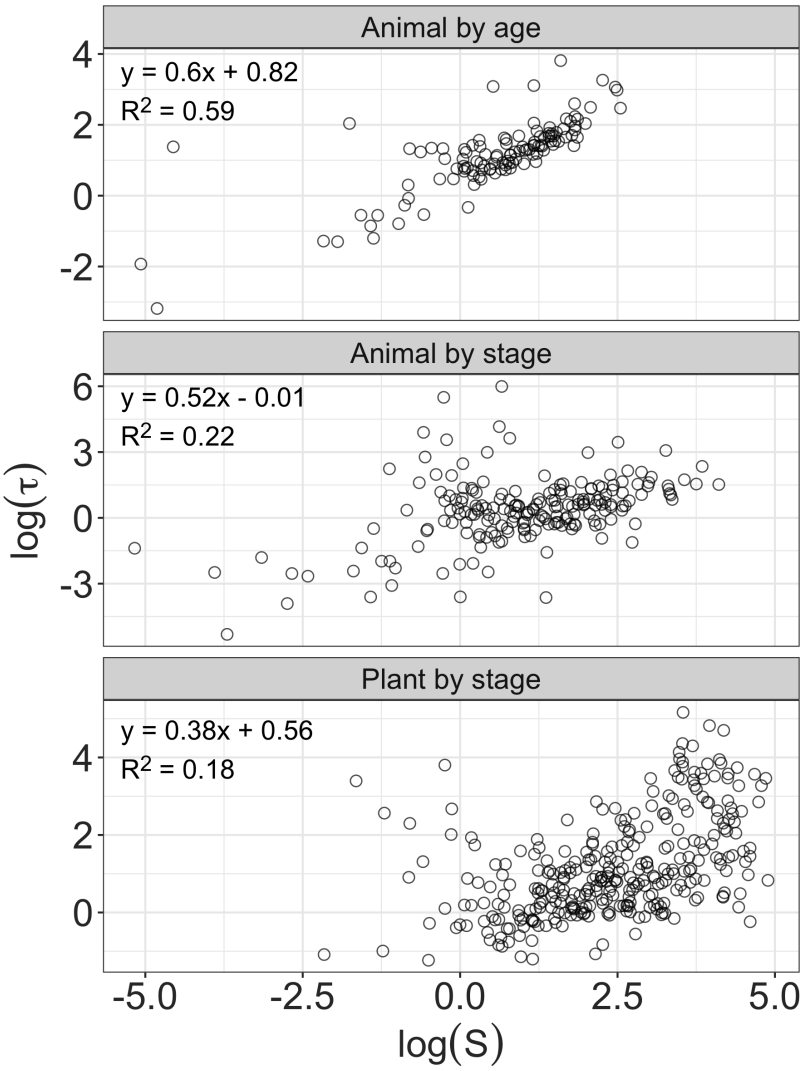

Figure C.7: Damping time (τ) versus reproductive dispersion (S) on a log-log scale. Time unit is years. Upper panel, age-structured animal data from COMADRE and GO; middle panel, stage-structured animal data from COMADRE; bottom panel, stage-structured plant data from COMPADRE. Each panel displays the fitted model and its coefficient of determination (R^2) based on PGLS regression. P-value in each panel is less than 0.001. The 95% confidence interval for the regression slope is [0.56, 0.65] for the upper panel, [0.45, 0.59] for the middle panel and [0.33, 0.42] for the bottom panel. Pagel's λ is 0.00, 0.14 and 0.52 for the upper, middle and bottom panels respectively.

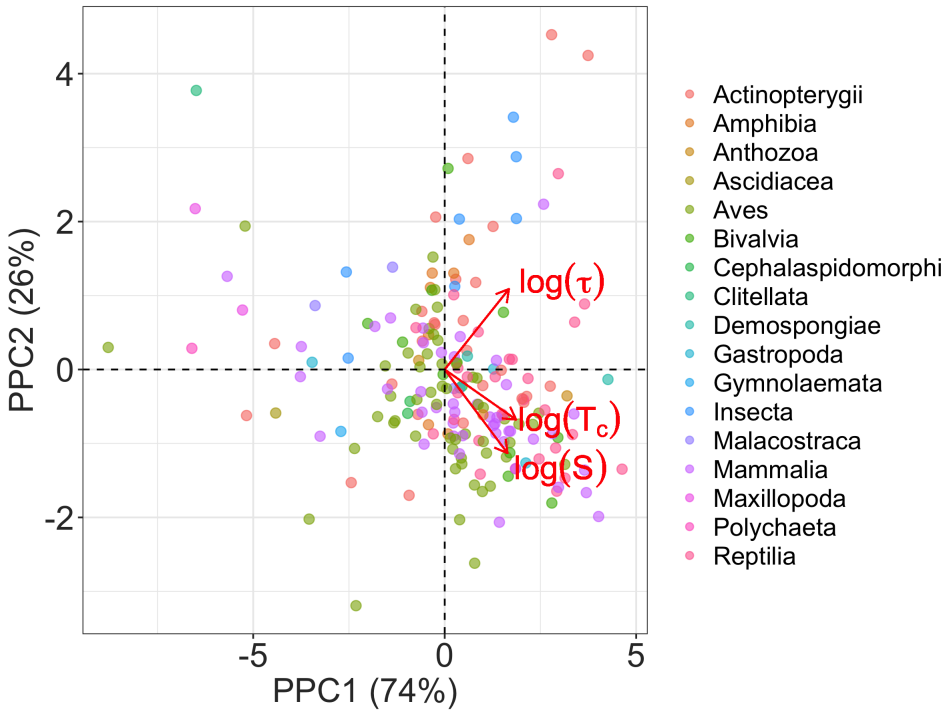

Figure C.8: Phylogenetic principal component analysis (PPCA) of reproductive dispersion (S), generation time (T_c) and damping time (τ) on a log scale for stage-structured animals. Arrow length indicates the loading of each life-history trait onto PCA axes. Points represent the position of species along the phylogeneticly corrected principal component (PPC)1 and 2 and are colored by Class. Numbers in parentheses on both axes represent the proportion of variance explained by the corresponding PPC.

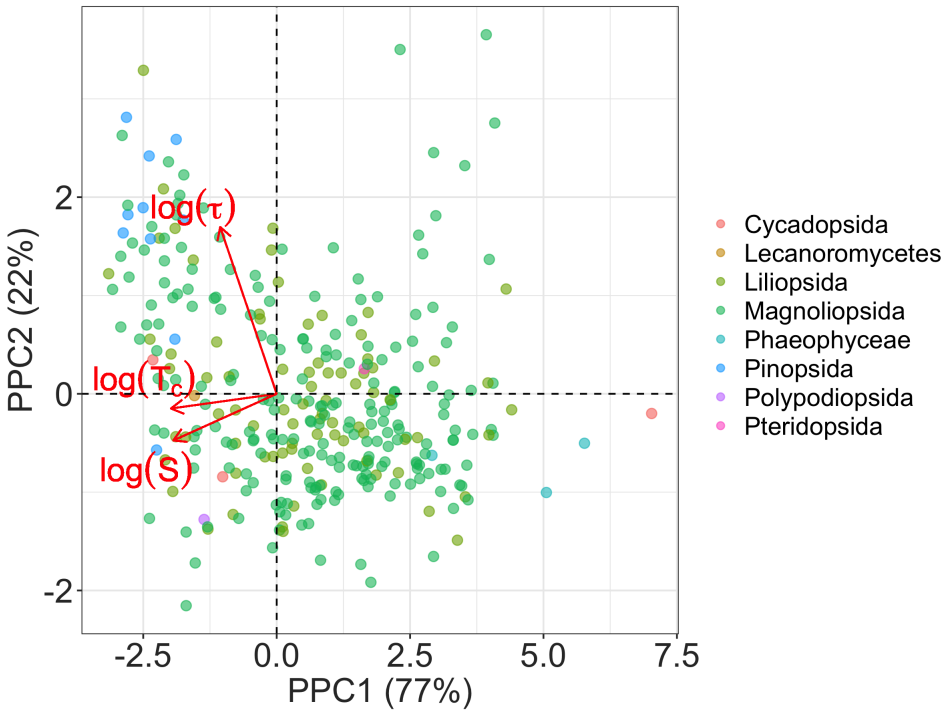

Figure C.9: Phylogenetic principal component analysis (PPCA) of reproductive dispersion (S), generation time (T_c) and damping time (τ) on a log scale for stage-structured plants. Arrow length indicates the loading of each life-history trait onto PCA axes. Points represent the position of species along the phylogeneticly corrected principal component (PPC)1 and 2 and are colored by Class. Numbers in parentheses on both axes represent the proportion of variance explained by the corresponding PPC.

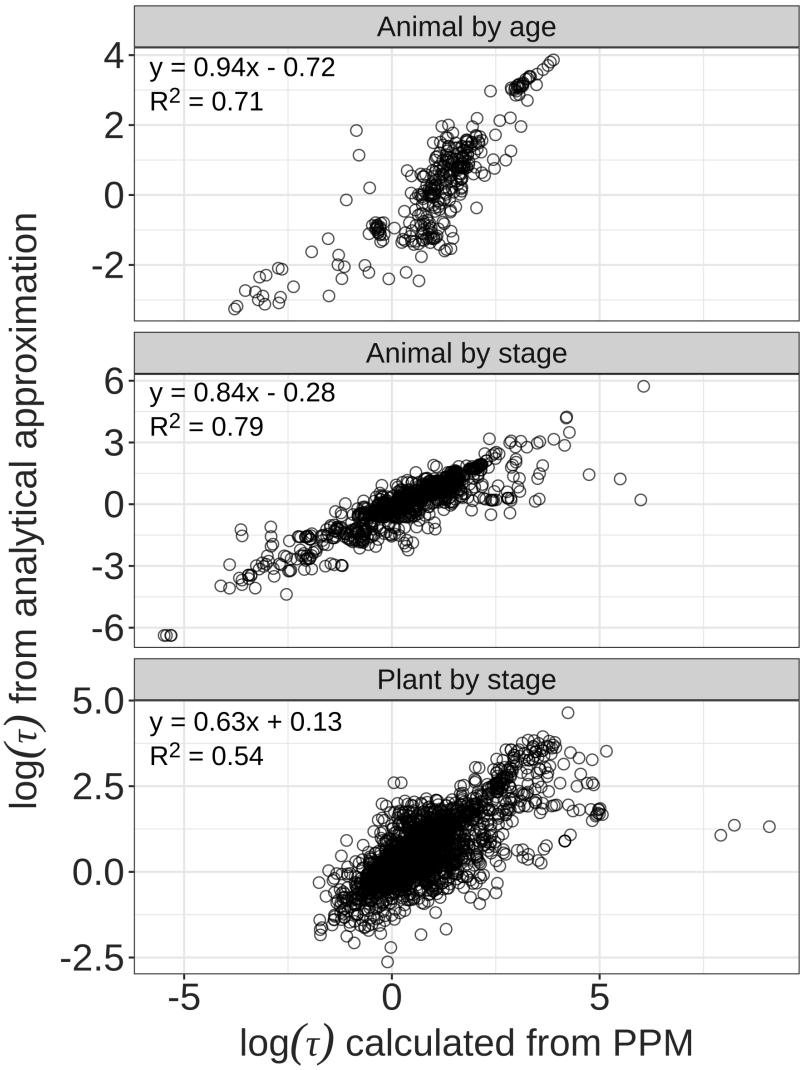

Figure C.10: Comparison between $\log(\tau)$ calculated from population projection matrix (PPM) and $\log(\tau)$ from analytical approximation. Noted that here we include results from 3865 matrices (689 different species). The unit of time is years. Specifically, there are age-structured animal data from COMADRE and GO (*upper*), stage-structured animal data from COMADRE (*middle*), and stage-structured plant data from COMPADRE (*bottom*). On the top left of each panel, we also present the fitted model and its coefficient of determination (R^2) based on ordinary least squares regression (OLS). The 95% confidence interval for the regression slope of each panel is: [0.91, 0.97] for the upper panel, [0.83, 0.85] for the middle panel and [0.62, 0.64] for the bottom panel.